

Multiplexed communication over a high-speed quantum channel

M. Heurs,¹ J. G. Webb,¹ A. E. Dunlop,¹ C. C. Harb,¹ T. C. Ralph,² and E. H. Huntington^{1,*}¹*Centre for Quantum Computer Technology, School of Information Technology and Electrical Engineering, University College, The University of New South Wales, Canberra, Australian Capitol Territory 2600, Australia*²*Centre for Quantum Computer Technology, Department of Physics, The University of Queensland, St. Lucia, Brisbane, Queensland 4072, Australia*

(Received 18 June 2009; published 25 March 2010)

In quantum information systems it is of particular interest to consider the best way in which to use the nonclassical resources consumed by that system. Quantum communication protocols are integral to quantum information systems and are among the most promising near-term applications of quantum information science. Here we show that a multiplexed, digital quantum communications system supported by a comb of vacuum squeezing has a greater channel capacity per photon than a source of broadband squeezing with the same analog band width. We report on the time-resolved, simultaneous observation of the first dozen teeth in a 2.4-GHz comb of vacuum squeezing produced by a subthreshold optical parametric oscillator, as required for such a quantum communications channel. We also demonstrate multiplexed communication on that channel.

DOI: [10.1103/PhysRevA.81.032325](https://doi.org/10.1103/PhysRevA.81.032325)

PACS number(s): 03.67.Hk, 42.50.Ex, 42.50.Dv, 42.65.Lm

I. INTRODUCTION

Quantum information science lies at the nexus of quantum mechanics and information science [1]. Quantum information systems will most likely comprise quantum information processing nodes connected by quantum communication channels [2] on which quantum communication protocols, such as quantum key distribution [3,4], quantum dense coding [5,6], and quantum teleportation [7,8], can be implemented [9–14]. A particularly important question in quantum information is how to make the best use of the quantum resources available, given the constraints of the system and its expected use (e.g., [15]). Here we consider the issue of making the best use of quantum resources in the context of high-capacity, multiplexed quantum communications.

One particularly useful optical nonclassical state for quantum communications is the squeezed vacuum [16,17]. The squeezed vacuum exhibits reduced noise relative to a classical channel in one measurement quadrature, at the cost of increased noise in the orthogonal quadrature. Simple passive operations can create entanglement, a key quantum resource, from squeezed vacua. With the addition of photon counting, other key resource states such as single photons [18] and cat states [19] can be heralded from squeezed vacua. Hence the study of quantum channels based on squeezed vacuum states can lead to a quite general understanding of the requirements of quantum communication channels. Here we produce and analyze such a channel.

Despite its name, a squeezed vacuum actually carries photons [20]. So the spectral properties of the squeezed vacuum must be well matched to the digital signaling scheme to avoid consuming nonclassical resources (i.e., photons) unnecessarily. Irrespective of the details of the coding protocol, contemporary digital communication schemes must all allow multiple users to have access to a high-capacity channel without experiencing interference from other users [21].

We show theoretically that a comb of squeezing can support a greater multiplexed channel capacity per photon than a source of broadband squeezing with the same analog bandwidth. We report on the time-resolved, simultaneous observation of the first dozen teeth in a >2.4-GHz comb of vacuum squeezing produced by a subthreshold optical parametric oscillator (OPO) and we demonstrate frequency-division multiplexed (FDM) communication on that channel. Combs of squeezing have been shown to be useful as the basic resource in creating cluster states for one-way quantum computing with continuous variables [22], but here we focus on their utility as a resource for quantum communication protocols.

II. THEORY

The Shannon capacity [23] of a communication channel with Gaussian noise (signal) of variance V_n (V_s) operating at the bandwidth limit is

$$C = \frac{1}{2} \log_2[1 + (V_s/V_n)]. \quad (1)$$

Equation (1) can be used to calculate the channel capacities of quantum states with Gaussian probability distributions [24,25].

The quality of a quantum channel is quantified by the bandwidth-limited channel capacity for a given consumption of nonclassical resources, in this case, photon number. The mean photon number per bandwidth per second of a light beam is related to the normalized variances in both the amplitude (V^+) and the phase (V^-) quadratures [26] as

$$\bar{n}(\omega) = \frac{1}{4}[V^+(\omega) + V^-(\omega) - 2]. \quad (2)$$

The variance in the encoded quadrature is $V_{ne} = V^- + V_s$, while the variance in the unencoded quadrature is $V_{nu} = 1/V^-$, assuming minimum uncertainty states and phase quadrature encoding.

We are interested in determining the maximum channel capacity for a given mean photon flux in the physical channel. The mean photon flux is given by $\Phi = \int \bar{n}(\omega)d\omega$ and may be combined with Eq. (1), Eq. (2), and the power spectral densities

*e.huntington@adfa.edu.au

of the squeezing and signal spectra to find the channel capacity for a given mean photon flux.

To the signal spectrum first. Multiple users can be given multiplexed access to a digital communications channel via either time-division multiplexing (TDM) or FDM [27]. In TDM, individual users are given access to the channel in specific time slots, with guard intervals between each use of the channel. In FDM, individual users are given access to specific-frequency subbands within the channel for the duration of their access to the channel, with guard bands between each subband. The guard intervals (bands) for TDM (FDM) ensure that there is no cross talk between users. Assuming that the channel is under more or less continuous use, the signal spectrum in a multiplexed, low-cross-talk, digital quantum communications system will be a continuous-wave frequency comb [21,27].

First consider the usual situation of squeezing, which is spectrally white over the analog bandwidth of the quantum channel. The signal spectrum will be a cw frequency comb, so

$$\begin{aligned}\Phi &= \frac{1}{4} \int d\omega \{V_s + [(V^- - 1)^2/V^-]\} \\ &= \frac{1}{4} \{B_s \tilde{V}_s + [B(\tilde{V}^- - 1)^2/\tilde{V}^-]\},\end{aligned}\quad (3)$$

where the normalized power spectral densities of the signal and noise are $V_s = \tilde{V} f(\omega)$ and $V^- = \tilde{V}^-$. The function $f(\omega)$ represents the comblike nature of the signal spectrum. We define B_s to be the integrated bandwidth consumed by the digital signaling scheme. The analog bandwidth of the quantum channel is $B \geq B_s$.

The maximum signal-to-noise for a given Φ will be $\tilde{V}_s/\tilde{V}^- = 4(\Phi^2 + \Phi B)/(B B_s)$, and the capacity for the quantum channel supported by a white squeezing spectrum is

$$C_{\text{white}} = \frac{1}{2} \log_2[(B B_s + 4\Phi^2 + 4\Phi B)/(B B_s)].\quad (4)$$

Now consider the situation in which the squeezing spectrum is matched to the signal spectrum (i.e., the squeezing spectrum also has a comb structure) so that $V^- = \tilde{V}^- f(\omega)$, and thus,

$$\Phi = \frac{1}{4} \{ \tilde{V}_s + [(\tilde{V}^- - 1)^2/\tilde{V}^-] \} B_s.\quad (5)$$

For Eq. (5), the maximum signal-to-noise ratio for a given Φ in the channel is $\tilde{V}_s/\tilde{V}^- = 4(\Phi^2 + \Phi B_s)/B_s^2$, which occurs at the optimum level of squeezing $\tilde{V}_{\text{opt}}^- = B_s/(B_s + 2\Phi)$. This leads to the following capacity:

$$C_{\text{comb}} = \log_2 [1 + (2\Phi/B_s)].\quad (6)$$

The channel capacity for a comb of squeezing is always greater than that for a white squeezing spectrum when constrained to the same photon flux.

Equation (6) is the standard result for a squeezed channel [25]. Comparison between Eq. (4) and Eq. (6) shows that the ‘‘standard result’’ is in fact the optimum squeezed channel capacity, achieved only when the signal and squeezing spectra are perfectly matched.

When restricted to homodyne detection, the optimum squeezed channel capacity is always greater than the capacity of the coherent-state (i.e. classical) channel with the same bandwidth and photon flux. In the notation used here, the coherent-state channel capacity with homodyne detection is $C_{\text{coh}} = \log_2[\sqrt{1 + (4\Phi/B_s)}]$ [24]. It has been shown that

communications systems using coherent states and optimal detection schemes can exceed C_{coh} , but as yet there is no known realization for those detection schemes (see Ref. [28] and references therein). We have restricted the analysis presented here to homodyne detection, for which there is an established experimental realization [25] and which therefore can be tested experimentally using current technology.

The ultimate capacity of a quantum communications channel exceeds the squeezed channel capacity and is set by the Holevo bound [25]. The Holevo-bounded channel capacity can be achieved using Fock states and photon number detection [25]. Dense coding systems constructed from squeezed vacuum sources can meet and even exceed the Holevo bound under experimentally realistic levels of squeezing and purity [24]. One observation to be made from the analysis herein is that the conclusions from previous analyses of dense coding capacities still stand, but only if the signal and squeezing spectra are well matched.

The output of a subthreshold OPO has been predicted theoretically to exhibit precisely the required spectral characteristics [29]. Frequency-resolved measurements of the first three resonances of an OPO were measured in Ref. [30] and subsequent measurements indicated that such systems could exhibit useful squeezing at many more resonances and used simultaneously. Here we present time-resolved, simultaneous measurements of the first dozen teeth in the comb of squeezing produced by a subthreshold OPO, as required for a high-speed multiplexed digital quantum communications channel.

Generalizing the result from Ref. [29] to include losses, the quadrature fluctuations for the channel as a function of angular frequency ω are

$$\delta X_{\text{out}}^\mp = \frac{[2\kappa_{\text{in}} - \kappa \mp \chi + (\frac{1-e^{i\omega\tau}}{\tau})] \delta X_{\text{in}}^\pm + 2\sqrt{\kappa_{\text{in}}\kappa_l} \delta X_l^\pm}{\kappa \pm \chi - (\frac{1-e^{i\omega\tau}}{\tau})},\quad (7)$$

where the cavity decay rate is $\kappa = \kappa_{\text{in}} + \kappa_l$ for $\kappa_{\text{in}} = T/\tau$ and $\kappa_l = L/\tau$. The cavity round-trip time is τ and the phase-matching bandwidth of the crystal is taken to be large compared to $1/\tau$. The nonlinear frequency conversion rate is $\chi = 2\beta_{\text{in}}\chi^{(2)}$, where $\chi^{(2)}$ is the second-order coefficient of nonlinearity for the nonlinear material and β_{in} is the amplitude of the pump field (assumed to be real without loss of generality).

Here the OPO output phase (δX_{out}^-) and amplitude (δX_{out}^+) quadrature fluctuations set the noise floor in the encoded and unencoded quadratures, respectively. The variances of the amplitude and phase quadratures, normalized to the quantum noise limit (QNL), are found from $V(\omega) = |\delta X(\omega)|^2$. Resonances in the squeezing spectrum are separated in frequency by the cavity free-spectral range, and we can think of each squeezing resonance as contributing to the quantum channel.

III. EXPERIMENT

Figure 1 illustrates the experiment schematically. The 532-nm, frequency-doubled output of a diode-pumped,

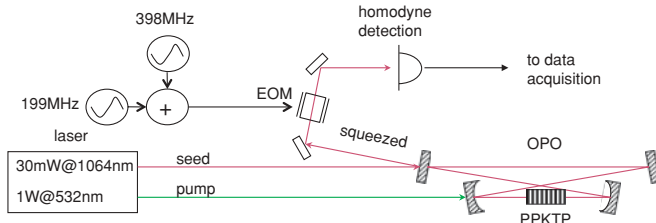


FIG. 1. (Color online) Schematic of experiment.

miniature monolithic Nd:YAG laser is used to pump a subthreshold OPO. The nonlinear crystal is periodically poled potassium titanyl phosphate, with a phase-matching temperature of 33.5°C . The OPO has a free-spectral range of 199 MHz and is operated with a parametric amplification of 3.9 dB and deamplification of 2.6 dB. A small fraction of the source laser power is tapped off prior to frequency doubling and is used as the seed to the OPO and the local oscillator for the homodyne measurements

The output of the OPO is sent to a homodyne detection system with an analog bandwidth of 2.5 GHz. The homodyne measurement is digitally sampled at 8 GS/s, which is sufficient for time-resolved homodyne detection. For the purposes of producing a frequency-resolved view, the discrete Fourier transforms of 12 207 time-resolved measurements of $1.024\text{-}\mu\text{s}$ duration are computed and their magnitudes averaged. The resulting frequency spectrum is shown in Fig. 2. The variances of the squeezed and anti-squeezed output of the OPO are shown relative to the measured quantum noise limit. The first dozen teeth in the comb of squeezing are clearly shown in Fig. 2.

We illustrate the principle of multiplexed communication on the quantum channel by implementing FDM over the first two resonances of the squeezing spectrum. Two independent sinusoids are generated, combined electrically, and used to phase modulate the OPO output as illustrated

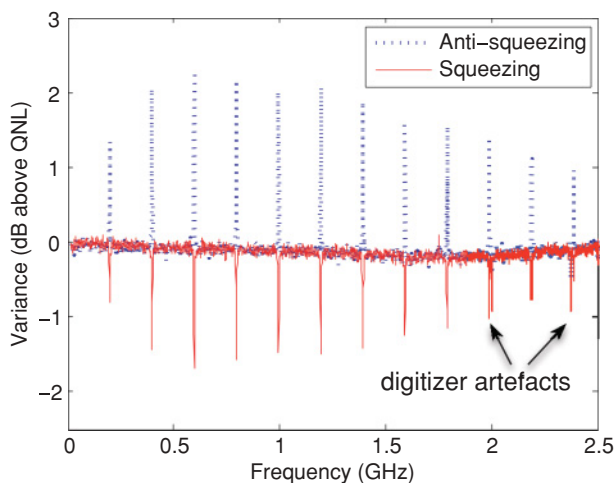


FIG. 2. (Color online) Averaged discrete Fourier transform of time-resolved quadrature homodyne measurement of squeezing comb. Artifacts arise from the frequency response of data acquisition.

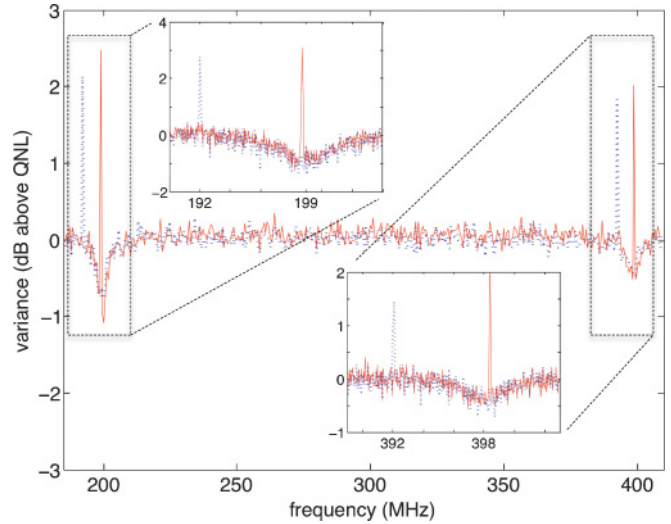


FIG. 3. (Color online) Measurements of FDM communications over the first and second resonances of the squeezing comb.

in Fig. 1. Subsequent detection and analysis complete the scheme. Figure 3 shows the measured frequency spectrum of the scheme. The solid (dashed) trace shows measurements relative to the quantum noise limit when the carrier frequencies are (are not) aligned with the resonances in the squeezing spectrum, 199 and 398 MHz (192 and 392 MHz), respectively. The improved signal-to-noise ratio ($V_s/V_n \approx 1.46$ vs $V_s/V_n \approx 1$), and hence channel capacity ($C \approx 0.65$ vs $C \approx 0.5$), when the signaling and squeezing spectra are aligned is clearly shown. The insets in Fig. 3 show a separate zoomed-in view of each independent frequency band.

IV. CONCLUSION

In summary, we have reported on time-resolved, simultaneous observation of the first dozen teeth in a 2.4-GHz comb of vacuum squeezing produced by a subthreshold OPO, and demonstrated multiplexed communications on that channel. We have shown theoretically that a quantum communications channel supported by such a comb of vacuum squeezing would have a greater channel capacity per photon than one supported by a source of broadband squeezing with the same analog bandwidth. These arguments carry over directly to the multiplexed distribution of quantum entanglement. If we consider quantum communication protocols that include photon counting, then our system has the added advantage of producing well-resolved frequency modes that can be cleanly separated through optical means and distributed to different photon counting modules.

ACKNOWLEDGMENT

This work was supported by the Australian Research Council.

- [1] M. A. Nielsen and I. L. Chuang, *Quantum Computation and Quantum Information* (Cambridge University Press, Cambridge, 2000).
- [2] H. J. Kimble, *Nature* **453**, 1023 (2008).
- [3] C. H. Bennett and G. Brassard, in *Proceedings of IEEE International Conference on Computers, Systems and Signal Processing, Bangalore, India* (IEEE, New York, 1984), pp. 175–179.
- [4] F. Grosshans and P. Grangier, *Phys. Rev. Lett.* **88**, 057902 (2002).
- [5] C. H. Bennett and S. J. Wiesner, *Phys. Rev. Lett.* **69**, 2881 (1992).
- [6] S. L. Braunstein and H. J. Kimble, *Phys. Rev. A* **61**, 042302 (2000).
- [7] C. H. Bennett, G. Brassard, C. Crepeau, R. Jozsa, A. Peres, and W. K. Wootters, *Phys. Rev. Lett.* **70**, 1895 (1993).
- [8] S. L. Braunstein and H. J. Kimble, *Phys. Rev. Lett.* **80**, 869 (1998).
- [9] W. T. Buttler, R. J. Hughes, P. G. Kwiat, S. K. Lamoreaux, G. G. Luther, G. L. Morgan, J. E. Nordholt, C. G. Peterson, and C. M. Simmons, *Phys. Rev. Lett.* **81**, 3283 (1998).
- [10] A. M. Lance, T. Symul, V. Sharma, C. Weedbrook, T. C. Ralph, and P. K. Lam, *Phys. Rev. Lett.* **95**, 180503 (2005).
- [11] K. Mattle, H. Weinfurter, P. G. Kwiat, and A. Zeilinger, *Phys. Rev. Lett.* **76**, 4656 (1996).
- [12] J. Mizuno, K. Wakui, A. Furusawa, and M. Sasaki, *Phys. Rev. A* **71**, 012304 (2005).
- [13] D. Bouwmeester *et al.*, *Nature (London)* **390**, 575 (1997).
- [14] A. Furusawa, J. L. Sorensen, S. L. Braunstein, C. A. Fuchs, H. J. Kimble, and E. S. Polzik, *Science* **282**, 706 (1998).
- [15] D. E. Browne and T. Rudolph, *Phys. Rev. Lett.* **95**, 010501 (2005).
- [16] U. L. Andersen and G. Leuchs, in *Lectures on Quantum Information*, edited by D. Bruss and G. Leuchs (Wiley-VCH, Berlin, 2007), Chap. 7.
- [17] H. Vahlbruch, S. Chelkowski, K. Danzmann, and R. Schnabel, *New J. Phys.* **9**, 371 (2007).
- [18] A. I. Lvovsky, H. Hansen, T. Aichele, O. Benson, J. Mlynek, and S. Schiller, *Phys. Rev. Lett.* **87**, 050402 (2001).
- [19] A. Ourjoumtsev, H. Jeong, R. Tualle-Brouiri, and P. Grangier, *Nature* **448**, 784 (2007).
- [20] D. F. Walls and G. J. Milburn, *Quantum Optics* (Springer-Verlag, Berlin, 1994).
- [21] B. Sklar, *IEEE Signal Process. Mag.* **87**, 19 (2003).
- [22] H. Zaidi *et al.*, *Laser Phys.* **18**, 659 (2008).
- [23] C. E. Shannon, *Bell Syst. Tech. J.* **27**, 623 (1948).
- [24] T. C. Ralph and E. H. Huntington, *Phys. Rev. A* **66**, 042321 (2002).
- [25] C. M. Caves and P. D. Drummond, *Rev. Mod. Phys.* **66**, 481 (1994).
- [26] T. C. Ralph, W. J. Munro, and R. E. S. Polkinghorne, *Phys. Rev. Lett.* **85**, 2035 (2000).
- [27] B. P. Lathi, *Modern Digital and Analog Communication Systems*, 2nd ed. (Oxford University Press, New York, 1995).
- [28] J. H. Shapiro, *J. Special Topics Quantum Electronics* **15**, 1547 (2009).
- [29] A. E. Dunlop, E. H. Huntington, C. C. Harb, and T. C. Ralph, *Phys. Rev. A* **73**, 013817 (2006).
- [30] R. J. Senior *et al.*, *Optics Express* **15**, 5310 (2007).
- [31] A. E. Dunlop (unpublished data, 2008).